

---

# MOVEMENT-PREDICTION-ADJUSTED NAÏVE FORECAST

---

Cheng Zhang<sup>†</sup>  
zcheng582dx@gmail.com

## ABSTRACT

This study introduces a movement-prediction-adjusted naïve forecast, which is the original naïve forecast with the addition of a weighted movement prediction term, in the context of forecasting time series that exhibit symmetric random walk properties. The weight of the movement term is determined by two parameters: one reflecting the directional accuracy and the other representing the mean absolute increment. The settings of the two parameters involve a trade-off: larger values may yield meaningful gains over the original naïve forecast, whereas smaller values often render the adjusted forecast more reliable. This trade-off can be managed by empirically setting the parameters using sliding windows on in-sample data. To statistically test the performance of the adjusted naïve forecast under different directional accuracy levels, we used four synthetic time series to simulate multiple forecast scenarios, assuming that for each directional accuracy level, diverse movement predictions were provided. The simulation results show that as the directional accuracy increases, the error of the adjusted naïve forecast decreases. In particular, the adjusted naïve forecast achieves statistically significant improvements over the original naïve forecast, even under a low directional accuracy of slightly above 0.50. This finding implies that the movement-prediction-adjusted naïve forecast can serve as a new optimal point forecast for time series with symmetric random walk characteristics if consistent movement prediction can be provided.

**Keywords** Naïve forecast · Movement prediction · Point forecasting · Symmetric random walk

## 1 Introduction

Time series forecasting plays a crucial role in many decision-making processes. The widespread demand for accurate point forecasts across various domains has attracted considerable attention from researchers and practitioners. However, not all time series are equally predictable. Time series exhibiting random walk characteristics pose significant forecasting challenges (Hamilton, 2020). Therefore, financial time series, known for these characteristics and their practical importance in financial markets, have been extensively studied as test cases for forecasting theories and methods. One prominent theory is the efficient market hypothesis (EMH), which suggests that asset prices incorporate all available information, rendering historical prices unpredictable (Fama, 1970). For a random walk-like series, the naïve forecast, which assumes that the future value at the next time step is equal to the current value, is often regarded as the optimal point forecast.

In support of the EMH, Moosa (2013) reported that as the volatility of financial time series increases, the root mean square error (RMSE) of the forecasting models increases more quickly than that of the naïve forecast. Moreover, Moosa and Burns (2014) argued that claims of outperforming the naïve forecast in terms of the RMSE are often misleading, frequently involving introduced dynamics without rigorous statistical validation. Despite attempts to use various predictors to break the assumed randomness of financial time series, existing forecasting methods, including statistical, machine learning, and deep learning approaches, typically cannot outperform naïve forecasts (Kilian and Taylor, 2003; Moosa and Burns, 2016; Thakkar and Chaudhari, 2021; Petropoulos et al., 2022; Ellwanger and Snudden, 2023; Hewamalage et al., 2023; Zeng et al., 2023; Beck et al., 2025).

<sup>†</sup>: <https://orcid.org/0000-0002-4150-3371>

From the forecaster's perspective, the unpredictability of random walk-like series could be attributed to incomplete knowledge of the underlying processes controlling the data, ignorance of the various contributing factors, and imperfections in analytical methods (Laplace, 2012). In other words, the randomness of data is not inherent but rather apparent (Crutchfield and Feldman, 2003). Although useful information may be contained in the input space, it can be overwhelmed by irrelevant data, making it difficult for current regression methods to exploit such information (John et al., 1994; Guyon and Elisseeff, 2003; Verleysen and François, 2005). Moreover, identifying the predictors on which the target variable truly depends is a complex task (Granger, 1969; Stock and Watson, 2002). However, these theories and empirical evidence reveal only the practical difficulty of finding exploitable patterns; they do not eliminate the possibility of discovering any predictability in the data.

Given the challenge in the point forecasting of random walk-like series, many researchers have shifted their focus from point forecasting to movement prediction, which involves predicting whether the value is increasing or decreasing for the next time step. Consequently, the regression task was reduced to a binary classification task. For a pure random walk, the probability that future movement will increase or decrease is 0.5, and the mutual information between the predictors and the target is zero (Kraskov et al., 2004). If the mutual information is greater than zero, it indicates that there is some dependency between the predictors and the target (Cover and Thomas, 2012). Practically, this means that the predictors reduce the uncertainty of the binary outcome. Although this does not guarantee high predictive accuracy, it suggests that, theoretically, one can build a model that performs better than random guessing (Ircio et al., 2020). In contrast, for point forecasting in a random walk-like series, the continuous nature of the target means that the small gain in mutual information only marginally reduces the overall uncertainty and does not sufficiently narrow down the precise numerical result (Beraha et al., 2019).

Movement prediction is often considered easier than point forecasting in financial time series (Taylor, 2008; Moosa, 2013). Studies in the field of behavioral finance suggest that investor sentiment and psychology can lead to certain patterns (De Bondt and Thaler, 1985; Lee et al., 1991; Baker and Wurgler, 2007; Barberis et al., 1998), which could lead to mutual information between the sentiment predictors and the binary target being greater than zero and making future movements predictable. Therefore, sentiment indicators are often used to improve the directional accuracy in these tasks. For example, Weng et al. (2017) incorporated Google news counts and Wikipedia page views alongside historical data to predict the next day's movement of AAPL stock via support vector machines (SVMs), achieving up to 0.80 directional accuracy. Ma et al. (2023) proposed a multisource aggregated classification (MAC) method for the prediction of stock price movement, incorporating the numerical features and market-driven news sentiments of target stocks, as well as the news sentiments of their related stocks, and the directional accuracy can reach as high as 0.70. Wang et al. (2025) used multimodal data that included news data to train a hybrid model consisting of a long short memory network (LSTM) and transformer for the prediction of stock movement, and the directional accuracy fell within the range of 0.57–0.87. Depending on the complexity of the markets and availability of data, the directional accuracy of financial time series typically ranges between 0.55 and 0.80 (Bustos and Pomares-Quimbaya, 2020).

When a movement prediction is better than a random guess, it also indicates that the input data contain useful information that has been leveraged effectively to predict future movements. Borrowing the "less is more" principle from cognitive science, where reducing information complexity can lead to an improved cognitive process (Gigerenzer and Brighton, 2009), we can subsequently use the result of the movement prediction to generate the point forecast, using only the binary labels as an additional predictor along with the original naïve forecast, as shown in Figure 1. The binary labels can then be regarded as "verified predictors" for the target variable, and no more noise is introduced to affect the final point forecast. Unfortunately, the use of movement prediction results only to improve point forecasts remains unexplored in the forecasting community. Most studies either stopped at the movement prediction stage or used a direct regression approach to conduct point forecasting. Although it is often argued that, in many cases, compared with point forecasting, movement prediction is more important for decision-making (Sezer et al., 2020), the final decision generally still depends on the estimated value of the target variable. For example, in financial markets, the decision could be to trade at a specific price given a predicted future movement. Therefore, the decision maker actually conducted the classification-to-regression conversion, albeit implicitly. However, how and why movement prediction results can be systematically exploited to improve point forecasting in random walk-like series is largely unknown.

Under these conditions, this study aimed to explore the potential of using movement prediction to enhance point forecasting in random walk-like time series. In particular, the target variable is assumed to follow a symmetric random walk process, which is the basic type of random walk characterized by the absence of drift and equal probabilities of upward and downward movements (Ibe, 2014). By reformulating the symmetric random walk process to incorporate the future movement of the target variable, the point forecast can naturally be expressed as the original naïve forecast adjusted by movement prediction, which is referred to as the movement-prediction-adjusted naïve forecast. The weight applied to the movement term is determined by two parameters: one reflecting the directional accuracy and the other representing the mean absolute increment. The setting of these two parameters introduces an inherent trade-off and uncertainty into the prediction performance. Specifically, larger parameter values suggest potentially meaningful

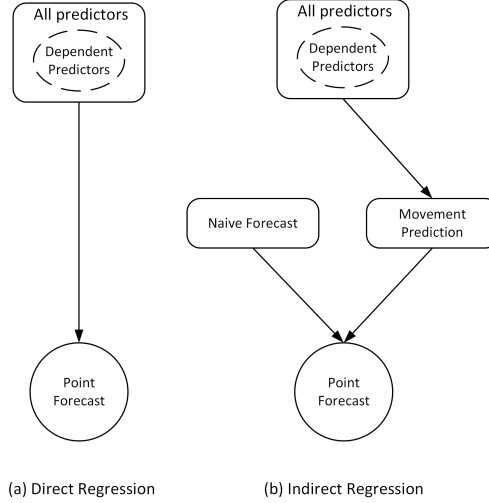


Figure 1: Direct and indirect regression approaches

improvements over the original naïve forecast, whereas smaller parameter values indicate a greater likelihood that the adjusted naïve forecast will outperform the original naïve forecast. To balance this trade-off, the parameters can be empirically determined by sliding windows on the in-sample data.

Since, in practice, movement prediction can exhibit a wide range of directional accuracies, the adjusted naïve forecast should be evaluated across different accuracy levels to examine the impact of directional accuracy on the performance of the proposed method. Therefore, we use synthetic time series to simulate multiple forecasting scenarios, assuming that for each directional accuracy level, diverse movement predictions are provided. For all the experiments, the evaluation metrics include the RMSE, mean absolute error (MAE), mean absolute percentage error (MAPE), and symmetric mean absolute percentage error (sMAPE), and the original naïve forecast serves as the sole baseline. In this experimental setting, it can be determined whether the improvement over the baseline by the proposed method is statistically significant.

This study makes three significant contributions to the literature. First, this study provides new insights into the predictability of random walk-like series, addressing a longstanding challenge in the field. When meaningful movement prediction was provided, the point values of the random walk-like series became partially predictable. Second, by illuminating the relationship between the actual and estimated parameter values, this study underscores the source of uncertainty in the effectiveness of the proposed method, a critical consideration often underemphasized by purely data-driven approaches. Third, the proposed method bridges movement prediction and point forecasting, which are two distinct tasks in time series forecasting. Although the use of binary classification to guide regression is well established, relying solely on the movement prediction of the target variable for its own point forecasting offers a fresh perspective.

The remainder of this paper is organized as follows. Section 2 introduces the details of the movement-prediction-adjusted naïve forecast, explains how to derive it, and explains why it can outperform the original naïve forecast. Section 3 presents a simulation study that assesses the performance of movement-prediction-adjusted naïve forecasts using synthetic datasets in a controlled experimental setting. Section 4 discusses the key findings, implications, and limitations of the study. Finally, Section 5 concludes the paper and outlines future research directions.

## 2 Movement-Prediction-Adjusted Naïve Forecast

This section presents the details of the movement-prediction-adjusted naïve forecast for time series that exhibit symmetric random walk characteristics. We first derive the general expression of the adjusted naïve forecast based on the definition of symmetric random walks, then explain how to optimize the parameters attached to the movement term, and finally, how to adjust the parameters to improve the forecasting effectiveness and detail the procedure for generating forecasts on the out-of-sample set.

## 2.1 General Expression

A symmetric random walk is a stochastic process in which the value at time step  $t$  is the sum of the value at the previous time step  $t - 1$  and the value of an independent random increment  $\epsilon_t$ , which is generally assumed to follow a normal distribution with a mean of 0 and variance of  $\sigma_t^2$  (De Gooijer et al., 2017). The formulation of symmetric random walks is as follows:

$$y_t = y_{t-1} + \epsilon_t, \epsilon_t \sim \mathcal{N}(0, \sigma_t^2), \quad (1)$$

where  $y_t$  is the point value at time step  $t$  and  $y_{t-1}$  is the point value at time step  $t - 1$ . For random walks exhibiting homoscedasticity, the variance  $\sigma_t^2$  remains constant over time, whereas for those exhibiting heteroscedasticity, the variance  $\sigma_t^2$  varies over time. The symmetric nature of the random increment  $\epsilon_t$  with a mean of 0 ensures that there is no inherent bias in the movement direction of the target variable and that upward and downward movements are equally likely (Ibe, 2014). Furthermore, the random increment  $\epsilon_t$  can be expressed as a product of two components: a nonnegative random increase  $|\epsilon_t|$  representing the magnitude of the increment and a sign component  $D_t$ , which takes a value of  $+1$  for upward movement and  $-1$  for downward movement, indicating the direction of the increment between two adjacent points. This allows the process to be reformulated as follows:

$$y_t = y_{t-1} + D_t \cdot |\epsilon_t|; |\epsilon_t| \geq 0 \quad (2)$$

The nonnegative random increment  $|\epsilon_t|$  can be further expressed as a product of two terms:

$$y_t = y_{t-1} + D_t \cdot \theta_t \cdot \bar{\epsilon}; \theta_t \geq 0, \bar{\epsilon} > 0, \quad (3)$$

where  $\bar{\epsilon}$  represents the mean absolute increment calculated from the in-sample data, which can be interpreted as a base magnitude of the increments. The term  $\theta_t$  is introduced as a nonnegative parameter that controls the magnitude of the increment at time step  $t$ . Eq. (3) implies that the point forecast of the target variable can be generated if  $D_t$  can be predicted and both  $\theta_t$  and  $\bar{\epsilon}$  can be estimated. Consider a simple scenario in which the magnitude of the increment between two adjacent points is fixed for future time steps; then,  $\theta_t$  can be set to a constant value. Consequently, the point forecast for future time step  $t$ , denoted as  $\hat{y}_t$ , can be expressed as follows:

$$\hat{y}_t = y_{t-1} + \hat{D}_t \cdot \theta \cdot \bar{\epsilon}; \bar{\epsilon} > 0, \quad (4)$$

where  $\hat{D}_t$  is the movement prediction,  $\theta$  is a fixed scalar, and  $\theta \in \mathbb{Q}$ . Therefore, the point forecast generated via Eq. (4) can be regarded as an adjustment of the original naïve forecast through a weighted movement prediction term; hence, it is named the movement-prediction-adjusted naïve forecast.

## 2.2 Movement Term Weight

According to Eq. (4), the weight of the movement term in the adjusted naïve forecast is the product of two parameters,  $\theta$  and  $\bar{\epsilon}$ , both of which can be estimated from the in-sample data. Since  $\bar{\epsilon}$  is directly computed as the mean absolute increment of the in-sample series, only  $\theta$  requires optimization. This is typically achieved by minimizing the mean squared error (MSE) of the adjusted naïve forecast for the in-sample set. Because the MSE of the original naïve forecast is a fixed value on the in-sample set, minimizing the MSE of the adjusted naïve forecast is mathematically equivalent to maximizing the difference between the MSEs of the original and adjusted naïve forecasts:

$$\min MSE_{\text{in-sample}}^{\text{adjusted-naïve}} \equiv \max \left( MSE_{\text{in-sample}}^{\text{original-naïve}} - MSE_{\text{in-sample}}^{\text{adjusted-naïve}} \right) \quad (5)$$

Using this approach, we can determine the optimal value of  $\theta$  and examine, through the difference between the MSEs, whether there is an improvement over the original naïve forecast under this optimal setting.

Suppose that the in-sample set has  $N$  time steps and that movement prediction  $\hat{D}_t$  is provided for each time step. Within the in-sample set, we assume that the movement prediction yields  $n_{\text{in-sample}}^{\text{correct}}$  correct and  $n_{\text{in-sample}}^{\text{incorrect}}$  incorrect directions. We subsequently used Eq. (2) to present the actual value and expand the MSE expression for the original naïve forecast:

$$\begin{aligned} MSE_{\text{in-sample}}^{\text{original-naïve}} &= \frac{1}{N} \left( \sum_{t \in \text{in-sample}} (y_t - y_{t-1})^2 \right) \\ &= \frac{1}{N} \left( \sum_{t \in \text{in-sample}} (y_{t-1} + D_t \cdot |\epsilon_t| - y_{t-1})^2 \right) \\ &= \frac{1}{N} \left( \sum_{t \in \text{correct}} |\epsilon_t|^2 + \sum_{t \in \text{incorrect}} |\epsilon_t|^2 \right) \end{aligned} \quad (6)$$

When using Eq. (2) to represent the actual value and Eq. (4) to represent the predicted value, the MSE of the adjusted naïve forecast on the in-sample set can be expressed as:

$$\begin{aligned}
 MSE_{\text{in-sample}}^{\text{adjusted-naïve}} &= \frac{1}{N} \left( \sum_{t \in \text{in-sample}} (y_t - \hat{y}_t)^2 \right) \\
 &= \frac{1}{N} \left( \sum_{t \in \text{correct}} (y_t - \hat{y}_t)^2 + \sum_{t \in \text{incorrect}} (y_t - \hat{y}_t)^2 \right) \\
 &= \frac{1}{N} \left( \sum_{t \in \text{correct}} \left[ (y_{t-1} + D_t \cdot |\epsilon_t|) - (y_{t-1} + \hat{D}_t \cdot \theta_{\text{in-sample}} \cdot \bar{\epsilon}_{\text{in-sample}}) \right]^2 \right. \\
 &\quad \left. + \sum_{t \in \text{incorrect}} \left[ (y_{t-1} + D_t \cdot |\epsilon_t|) - (y_{t-1} + \hat{D}_t \cdot \theta_{\text{in-sample}} \cdot \bar{\epsilon}_{\text{in-sample}}) \right]^2 \right) \\
 &= \frac{1}{N} \left( \sum_{t \in \text{correct}} (|\epsilon_t|^2 - 2 \cdot \theta_{\text{in-sample}} \cdot |\epsilon_t| \cdot \bar{\epsilon}_{\text{in-sample}} + \theta_{\text{in-sample}}^2 \cdot \bar{\epsilon}_{\text{in-sample}}^2) \right. \\
 &\quad \left. + \sum_{t \in \text{incorrect}} (|\epsilon_t|^2 + 2 \cdot \theta_{\text{in-sample}} \cdot |\epsilon_t| \cdot \bar{\epsilon}_{\text{in-sample}} + \theta_{\text{in-sample}}^2 \cdot \bar{\epsilon}_{\text{in-sample}}^2) \right), \tag{7}
 \end{aligned}$$

where  $\theta_{\text{in-sample}}$  represents the parameter  $\theta$  estimated from the in-sample set and  $\bar{\epsilon}_{\text{in-sample}}$  denotes the mean of  $|\epsilon_t|$  calculated over the in-sample set. Consequently, the difference between the two MSEs on the in-sample set can be derived via Eq. (6) and Eq. (7), respectively:

$$\begin{aligned}
 \Delta MSE_{\text{in-sample}} &= MSE_{\text{in-sample}}^{\text{original-naïve}} - MSE_{\text{in-sample}}^{\text{adjusted-naïve}} \\
 &= \frac{1}{N} \left( \sum_{t \in \text{correct}} |\epsilon_t|^2 + \sum_{t \in \text{incorrect}} |\epsilon_t|^2 \right) \\
 &\quad - \frac{1}{N} \left( \sum_{t \in \text{correct}} (|\epsilon_t|^2 - 2 \cdot \theta_{\text{in-sample}} \cdot |\epsilon_t| \cdot \bar{\epsilon}_{\text{in-sample}} + \theta_{\text{in-sample}}^2 \cdot \bar{\epsilon}_{\text{in-sample}}^2) \right. \\
 &\quad \left. + \sum_{t \in \text{incorrect}} (|\epsilon_t|^2 + 2 \cdot \theta_{\text{in-sample}} \cdot |\epsilon_t| \cdot \bar{\epsilon}_{\text{in-sample}} + \theta_{\text{in-sample}}^2 \cdot \bar{\epsilon}_{\text{in-sample}}^2) \right) \\
 &= \frac{1}{N} \left( \sum_{t \in \text{correct}} (2 \cdot \theta_{\text{in-sample}} \cdot |\epsilon_t| \cdot \bar{\epsilon}_{\text{in-sample}} - \theta_{\text{in-sample}}^2 \cdot \bar{\epsilon}_{\text{in-sample}}^2) \right. \\
 &\quad \left. - \sum_{t \in \text{incorrect}} (2 \cdot \theta_{\text{in-sample}} \cdot |\epsilon_t| \cdot \bar{\epsilon}_{\text{in-sample}} + \theta_{\text{in-sample}}^2 \cdot \bar{\epsilon}_{\text{in-sample}}^2) \right) \tag{8}
 \end{aligned}$$

Based on the law of large numbers (LLN), when both  $n_{\text{in-sample}}^{\text{correct}}$  and  $n_{\text{in-sample}}^{\text{incorrect}}$  are sufficiently large, the following approximations hold:

$$\sum_{t \in \text{correct}} |\epsilon_t| \approx n_{\text{in-sample}}^{\text{correct}} \cdot \bar{\epsilon}_{\text{in-sample}}, \quad \sum_{t \in \text{incorrect}} |\epsilon_t| \approx n_{\text{in-sample}}^{\text{incorrect}} \cdot \bar{\epsilon}_{\text{in-sample}} \tag{9}$$

Therefore, Eq. (8) can be simplified as follows:

$$\begin{aligned}
 \Delta MSE_{\text{in-sample}} &= MSE_{\text{in-sample}}^{\text{original-naïve}} - MSE_{\text{in-sample}}^{\text{adjusted-naïve}} \\
 &\approx \frac{1}{N} \left( 2 \cdot \theta_{\text{in-sample}} \cdot \bar{\epsilon}_{\text{in-sample}} \cdot (n_{\text{in-sample}}^{\text{correct}} \cdot \bar{\epsilon}_{\text{in-sample}}) - n_{\text{in-sample}}^{\text{correct}} \cdot \theta_{\text{in-sample}}^2 \cdot \bar{\epsilon}_{\text{in-sample}}^2 \right. \\
 &\quad \left. - 2 \cdot \theta_{\text{in-sample}} \cdot \bar{\epsilon}_{\text{in-sample}} \cdot (n_{\text{in-sample}}^{\text{incorrect}} \cdot \bar{\epsilon}_{\text{in-sample}}) - n_{\text{in-sample}}^{\text{incorrect}} \cdot \theta_{\text{in-sample}}^2 \cdot \bar{\epsilon}_{\text{in-sample}}^2 \right) \\
 &= (4 \cdot \theta_{\text{in-sample}} \cdot ACC_{\text{in-sample}} - \theta_{\text{in-sample}}^2 - 2 \cdot \theta_{\text{in-sample}}) \cdot \bar{\epsilon}_{\text{in-sample}}^2, \tag{10}
 \end{aligned}$$

where  $ACC_{\text{in-sample}}$  is the directional accuracy of the movement prediction on the in-sample set, which is defined as:

$$ACC_{\text{in-sample}} = \frac{n_{\text{in-sample}}^{\text{correct}}}{n_{\text{in-sample}}^{\text{incorrect}} + n_{\text{in-sample}}^{\text{correct}}} \tag{11}$$

To maximize the  $\Delta MSE_{\text{in-sample}}$ , we focus on the expression inside parentheses in the final form of Eq. (10), which can be regarded as a function of parameter  $\theta_{\text{in-sample}}$ :

$$f(\theta_{\text{in-sample}}) = 4 \cdot \theta_{\text{in-sample}} \cdot ACC_{\text{in-sample}} - \theta_{\text{in-sample}}^2 - 2 \cdot \theta_{\text{in-sample}} \quad (12)$$

By differentiating  $f(\theta_{\text{in-sample}})$  and setting  $f'(\theta_{\text{in-sample}}) = 0$ , the critical value of  $\theta_{\text{in-sample}}$ , denoted as  $\theta_{\text{in-sample}}^*$ , is given by:

$$\theta_{\text{in-sample}}^* = 2 \cdot ACC_{\text{in-sample}} - 1 \quad (13)$$

Because  $f''(\theta_{\text{in-sample}}) < 0$ , the function  $f(\theta_{\text{in-sample}})$  is concave downward, and the critical point of  $f(\theta_{\text{in-sample}})$  is the maximum. Therefore,  $\theta_{\text{in-sample}}^*$  represents the optimal value of parameter  $\theta$  in the in-sample set. In addition, Eq. (13) reveals the relationship between the optimal value of parameter  $\theta$  and the directional accuracy of the movement prediction within a fixed sequence length. According to Eqs. (10) and (13), the improvement over the original naïve forecast on the in-sample set, achieved by the adjusted naïve forecast with optimal parameters, is expressed as follows:

$$\max \Delta MSE_{\text{in-sample}} = (\theta_{\text{in-sample}}^*)^2 \cdot \bar{\epsilon}_{\text{in-sample}}^2 \quad (14)$$

According to Eqs. (13) and (14), as the directional accuracy increases from 0.5, the value of  $f(\theta_{\text{in-sample}})$  increases from 0, and the improvement over the original naïve forecast correspondingly increases from 0. Because this improvement is a nonnegative value, the adjusted naïve forecast is at least as good as the original naïve forecast on the in-sample set:

$$MSE_{\text{in-sample}}^{\text{adjusted-naïve}} \leq MSE_{\text{in-sample}}^{\text{original-naïve}} \quad (15)$$

### 2.3 Forecast on the Out-of-Sample Set

If we use  $\theta_{\text{in-sample}}^*$  and  $\bar{\epsilon}_{\text{in-sample}}$  as the estimates of the actual optimal values of  $\theta$  and  $\bar{\epsilon}$  on the out-of-sample set and suppose that the movement prediction on the out-of-sample set with  $M$  time steps yields  $m_{\text{out-of-sample}}^{\text{correct}}$  correct directions and  $m_{\text{out-of-sample}}^{\text{incorrect}}$  incorrect directions; then, the difference between the two MSEs on the out-of-sample set can be expressed as follows:

$$\begin{aligned} \Delta MSE_{\text{out-of-sample}} &= MSE_{\text{out-of-sample}}^{\text{original-naïve}} - MSE_{\text{out-of-sample}}^{\text{adjusted-naïve}} \\ &= \frac{1}{M} \left( \sum_{t \in \text{correct}} |\epsilon_t|^2 + \sum_{t \in \text{incorrect}} |\epsilon_t|^2 \right) \\ &\quad - \frac{1}{M} \left( \sum_{t \in \text{correct}} \left( |\epsilon_t|^2 - 2 \cdot \theta_{\text{in-sample}}^* \cdot |\epsilon_t| \cdot \bar{\epsilon}_{\text{in-sample}} + (\theta_{\text{in-sample}}^*)^2 \cdot \bar{\epsilon}_{\text{in-sample}}^2 \right) \right. \\ &\quad \left. + \sum_{t \in \text{incorrect}} \left( |\epsilon_t|^2 + 2 \cdot \theta_{\text{in-sample}}^* \cdot |\epsilon_t| \cdot \bar{\epsilon}_{\text{in-sample}} + (\theta_{\text{in-sample}}^*)^2 \cdot \bar{\epsilon}_{\text{in-sample}}^2 \right) \right) \\ &= \frac{1}{M} \left( \sum_{t \in \text{correct}} \left( 2 \cdot \theta_{\text{in-sample}}^* \cdot |\epsilon_t| \cdot \bar{\epsilon}_{\text{in-sample}} - (\theta_{\text{in-sample}}^*)^2 \cdot \bar{\epsilon}_{\text{in-sample}}^2 \right) \right. \\ &\quad \left. - \sum_{t \in \text{incorrect}} \left( 2 \cdot \theta_{\text{in-sample}}^* \cdot |\epsilon_t| \cdot \bar{\epsilon}_{\text{in-sample}} + (\theta_{\text{in-sample}}^*)^2 \cdot \bar{\epsilon}_{\text{in-sample}}^2 \right) \right) \end{aligned} \quad (16)$$

Let  $\bar{\epsilon}_{\text{out-of-sample}}$  denote the actual mean absolute increment on the out-of-sample set. According to the LLN, when both  $m_{\text{out-of-sample}}^{\text{correct}}$  and  $m_{\text{out-of-sample}}^{\text{incorrect}}$  are sufficiently large, the following approximations hold:

$$\sum_{t \in \text{correct}} |\epsilon_t| \approx m_{\text{out-of-sample}}^{\text{correct}} \cdot \bar{\epsilon}_{\text{out-of-sample}}, \quad \sum_{t \in \text{incorrect}} |\epsilon_t| \approx m_{\text{out-of-sample}}^{\text{incorrect}} \cdot \bar{\epsilon}_{\text{out-of-sample}} \quad (17)$$

Therefore, Eq. (16) can further be expressed as:

$$\begin{aligned}
 \Delta MSE_{\text{out-of-sample}} &= MSE_{\text{out-of-sample}}^{\text{original-naïve}} - MSE_{\text{out-of-sample}}^{\text{adjusted-naïve}} \\
 &\approx \frac{1}{M} \left( 2 \cdot \theta_{\text{in-sample}}^* \cdot \bar{\epsilon}_{\text{in-sample}} \cdot (m_{\text{out-of-sample}}^{\text{correct}} \cdot \bar{\epsilon}_{\text{out-of-sample}}) - m_{\text{out-of-sample}}^{\text{correct}} \cdot (\theta_{\text{in-sample}}^*)^2 \cdot \bar{\epsilon}_{\text{in-sample}}^2 \right. \\
 &\quad \left. - 2 \cdot \theta_{\text{in-sample}}^* \cdot \bar{\epsilon}_{\text{in-sample}} \cdot (m_{\text{out-of-sample}}^{\text{incorrect}} \cdot \bar{\epsilon}_{\text{out-of-sample}}) - m_{\text{out-of-sample}}^{\text{incorrect}} \cdot (\theta_{\text{in-sample}}^*)^2 \cdot \bar{\epsilon}_{\text{in-sample}}^2 \right) \\
 &= 2 \cdot \theta_{\text{in-sample}}^* \cdot \bar{\epsilon}_{\text{in-sample}} \cdot ACC_{\text{out-of-sample}} \cdot \bar{\epsilon}_{\text{out-of-sample}} - 2 \cdot \theta_{\text{in-sample}}^* \cdot \bar{\epsilon}_{\text{in-sample}} \\
 &\quad \cdot (1 - ACC_{\text{out-of-sample}}) \cdot \bar{\epsilon}_{\text{out-of-sample}} - (\theta_{\text{in-sample}}^*)^2 \cdot \bar{\epsilon}_{\text{in-sample}}^2 \\
 &= 2 \cdot \theta_{\text{in-sample}}^* \cdot \bar{\epsilon}_{\text{in-sample}} \cdot \theta_{\text{out-of-sample}}^* \cdot \bar{\epsilon}_{\text{out-of-sample}} - (\theta_{\text{in-sample}}^*)^2 \cdot \bar{\epsilon}_{\text{in-sample}}^2,
 \end{aligned} \tag{18}$$

where  $ACC_{\text{out-of-sample}}$  is the directional accuracy of the movement prediction on the out-of-sample set, which is defined as:

$$ACC_{\text{out-of-sample}} = \frac{m_{\text{out-of-sample}}^{\text{correct}}}{m_{\text{out-of-sample}}^{\text{incorrect}} + m_{\text{out-of-sample}}^{\text{correct}}}, \tag{19}$$

and  $\theta_{\text{out-of-sample}}^*$  is the actual optimal value of  $\theta$  for the out-of-sample set, which is derived according to Eq. (13):

$$\theta_{\text{out-of-sample}}^* = 2 \cdot ACC_{\text{out-of-sample}} - 1 \tag{20}$$

To ensure the effectiveness of the adjusted naïve forecast, the  $\Delta MSE_{\text{out-of-sample}}$  should be no less than zero. Therefore, according to Eq. (18), the following inequality must be satisfied:

$$\theta_{\text{out-of-sample}}^* \cdot \bar{\epsilon}_{\text{out-of-sample}} \geq \frac{1}{2} \cdot \theta_{\text{in-sample}}^* \cdot \bar{\epsilon}_{\text{in-sample}} \tag{21}$$

Given that  $\theta_{\text{in-sample}}^*$  and  $\bar{\epsilon}_{\text{in-sample}}$  are specific estimates of  $\theta_{\text{out-of-sample}}^*$  and  $\bar{\epsilon}_{\text{out-of-sample}}$ , respectively, inequality (21) can be generalized as:

$$\theta_{\text{out-of-sample}}^* \cdot \bar{\epsilon}_{\text{out-of-sample}} \geq \frac{1}{2} \cdot \hat{\theta}_{\text{out-of-sample}} \cdot \hat{\bar{\epsilon}}_{\text{out-of-sample}}, \tag{22}$$

where  $\hat{\theta}_{\text{out-of-sample}}$  represents the estimate of  $\theta_{\text{out-of-sample}}^*$  and  $\hat{\bar{\epsilon}}_{\text{out-of-sample}}$  represents the estimate of  $\bar{\epsilon}_{\text{out-of-sample}}$ . Since the values of  $\theta_{\text{out-of-sample}}^*$  and  $\bar{\epsilon}_{\text{out-of-sample}}$  cannot be determined in advance, whether the inequality (22) can be satisfied is unknown, even when the optimal parameters derived from the in-sample set are used. Therefore, inequality (22) reveals the source of the uncertainty in the effectiveness of the adjusted naïve forecast, which depends on whether the product of the actual parameters exceeds half the product of the estimated parameters.

We can regard  $\theta_{\text{out-of-sample}}^*$  and  $\bar{\epsilon}_{\text{out-of-sample}}$  as two variables, each of which follows a distribution with a nonnegative range. Inequality (22) represents an event whose probability of occurrence depends on the estimated values of the two variables. When both estimates are set to small values near zero, the probability that inequality (22) is satisfied approaches one. However, in such a setting, the improvement over the original naïve forecast by the adjusted naïve forecast on the out-of-sample set also diminishes. Therefore, inequality (22) also reflects a trade-off between maximizing the probability that the adjusted naïve forecast outperforms the original forecast and achieving a meaningful level of improvement.

In addition to using  $\theta_{\text{in-sample}}^*$  and  $\bar{\epsilon}_{\text{in-sample}}$  as the estimates of  $\theta_{\text{out-of-sample}}^*$  and  $\bar{\epsilon}_{\text{out-of-sample}}$ , which may result in overfitting, a more conservative approach can be used to set the estimated values of  $\theta_{\text{out-of-sample}}^*$  and  $\bar{\epsilon}_{\text{out-of-sample}}$ :

1. Consider a data-generating process in which a sliding window, whose length is equal to that of the out-of-sample set, moves sequentially from the beginning to the end of the in-sample set. Each window can be treated as an "out-of-sample set" in the historical context.
2. Within each window, the directional accuracy is calculated and then translated into the corresponding value of  $\theta$  via Eq. (13). As the window moves, a collection of  $\theta$  values is generated, denoted as  $\Theta_{\text{set}}$ , whose bounds can be regarded as the estimated range of  $\theta_{\text{out-of-sample}}^*$ .
3. Similarly, a sliding window of the same length is applied to calculate a set of  $\bar{\epsilon}$  values from the in-sample set, denoted as  $\bar{\epsilon}_{\text{set}}$ , providing an estimated value range of  $\bar{\epsilon}_{\text{out-of-sample}}$ .
4. Using  $\min(\Theta_{\text{set}})$  and  $\min(\bar{\epsilon}_{\text{set}})$  as conservative estimates for  $\theta_{\text{out-of-sample}}^*$  and  $\bar{\epsilon}_{\text{out-of-sample}}$ , the adjusted naïve forecast for time step  $t$  in the out-of-sample set can be expressed as:

$$\hat{y}_t = y_{t-1} + \hat{D}_t \cdot \min(\Theta_{\text{set}}) \cdot \min(\bar{\epsilon}_{\text{set}}) \tag{23}$$

Algorithm 1 describes the process of generating the adjusted naïve forecast on the entire out-of-sample set.



---

**Algorithm 1** Movement-Prediction-Adjusted Naïve Forecast on the Out-of-sample Set
 

---

**Inputs:**  
 $Y_{\text{in-sample}}$  // Array of observations in the in-sample set  
 $Y_{\text{out-of-sample}}$  // Array of observations in the out-of-sample set  
 $\hat{D}_{\text{in-sample}}$  // Movement prediction on the in-sample set  
 $\hat{D}_{\text{out-of-sample}}$  // Movement prediction on the out-of-sample set  
 $N$  // Number of elements in the in-sample set  
 $M$  // Number of elements in the out-of-sample set  
**Output:**  
 $P$  // Adjusted naïve forecast on the out-of-sample set

- 1. Initialize variables:**  
 $D_{\text{in-sample}} \leftarrow []$  // Actual movements on the in-sample set  
 $P \leftarrow []$   
 $ACC_{\text{set}} \leftarrow []$  // Directional accuracy set  
 $\Theta_{\text{set}} \leftarrow []$  // Theta set  
 $R_{\text{in-sample}} \leftarrow []$  // First-order difference set  
 $\bar{\epsilon}_{\text{set}} \leftarrow []$  // Mean absolute increment set
- 2. Calculate actual movements:**  
**for**  $t \leftarrow 1$  to  $\text{length}(Y_{\text{in-sample}})$  **do**  
      $\text{diff} \leftarrow Y_{\text{in-sample}}[t] - Y_{\text{in-sample}}[t - 1]$  // First-order difference  
      $R_{\text{in-sample}}.\text{append}(\text{diff})$   
     **if**  $\text{diff} > 0$  **then**  
          $D_{\text{in-sample}}.\text{append}(1)$  // Upward movement  
     **else**  
          $D_{\text{in-sample}}.\text{append}(-1)$  // Downward or no movement  
     **end if**  
**end for**
- 3. Calculate directional accuracies:**  
**for**  $t \leftarrow 1$  to  $N - M + 1$  **do**  
      $\text{Correct\_Predictions} \leftarrow 0$   
     **for**  $i \leftarrow t$  to  $t + M - 1$  **do**  
         **if**  $D_{\text{in-sample}}[i] == \hat{D}_{\text{in-sample}}[i]$  **then**  
              $\text{Correct\_Predictions} \leftarrow \text{Correct\_Predictions} + 1$   
         **end if**  
     **end for**  
      $ACC_{\text{set}}.\text{append}(\text{Correct\_Predictions}/M)$   
**end for**
- 4. Compute the movement weights:**  
**for each**  $ACC \in ACC_{\text{set}}$  **do**  
      $\theta \leftarrow 2 \cdot ACC - 1$   
      $\Theta_{\text{set}}.\text{append}(\theta)$   
**end for**
- 5. Compute the mean absolute increments:**  
**for**  $t \leftarrow 1$  to  $N - M + 1$  **do**  
      $\bar{\epsilon} \leftarrow \text{mean}(|R_{\text{in-sample}}[t : t + M - 1]|)$   
      $\bar{\epsilon}_{\text{set}}.\text{append}(\bar{\epsilon})$   
**end for**
- 6. Set the initial forecast:**  
 $Y_{\text{last}} \leftarrow Y_{\text{in-sample}}[\text{end}]$  // Start from the last element of the in-sample set
- 7. Forecast the out-of-sample set:**  
**for**  $i \leftarrow 1$  to  $\text{length}(Y_{\text{out-of-sample}}) - 1$  **do**  
      $\Delta \leftarrow \min(\Theta_{\text{set}}) \cdot \min(\bar{\epsilon}_{\text{set}}) \cdot \hat{D}_{\text{out-of-sample}}[i]$  // Compute increment  
      $Y_{\text{forecast}} \leftarrow Y_{\text{last}} + \Delta$  // Compute the adjusted naïve forecast  
      $P.\text{append}(Y_{\text{forecast}})$  // Store result  
      $Y_{\text{last}} \leftarrow Y_{\text{out-of-sample}}[i]$   
**end for**
- 8. Return:**  
**return**  $P$

---



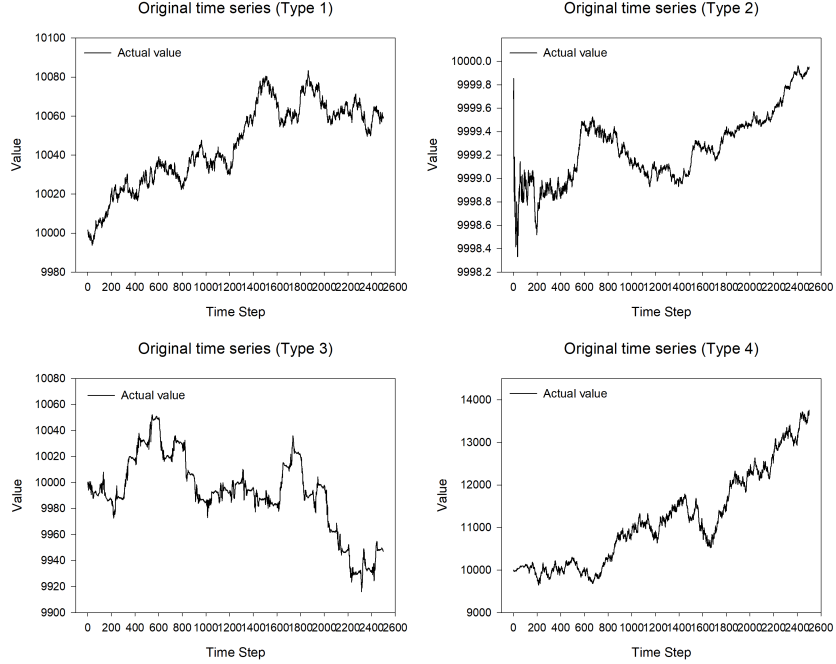


Figure 2: Synthetic time series: Type 1, constant variance ( $\sigma_0^2 = 1$ ); Type 2, linear variance trend ( $k = 4.95$ ); Type 3, cyclic variance ( $a = 7.77$ ); and Type 4, randomly varying variance ( $\xi^2 = 920$ ).

### 3 Simulation

This section presents a simulation study using four synthetic time series to evaluate whether the adjusted naïve forecast outperforms the original naïve forecast under different directional accuracy levels; therefore, movement prediction is assumed to have been provided. To statistically test the performance of the proposed method on an out-of-sample set, multiple movement predictions were randomly generated for each directional accuracy level.

#### 3.1 Datasets and Setup

The dataset includes four synthetic time series, each of which represents a symmetric random walk with a certain type of variance, as summarized in Table 1. Each time series, consisting of 2,500 steps, used a fixed random seed (seed = 1) in the Python environment, as shown in Figure 2. To maintain all values within the positive range, an initial positive offset of 10000 units was applied to each series. The last 500 data points were selected as the out-of-sample set, and the remaining data points were used as the in-sample set. In addition, Figure 3 shows the first-order differences of each time series to visually demonstrate the properties of the increments, and Figure 4 shows the histograms of the first-order differences for all time series, highlighting the symmetric nature of the time series.

Table 1: Synthetic time series summary

Variance Type	Expression	Parameter Range
Constant variance	$\sigma_t^2 = \sigma_0^2$	$\sigma_0^2 = 1$
Linear variance trend	$\sigma_t^2 = \frac{\sigma_0^2}{1+k \cdot t}$	$\sigma_0^2 = 1, k \in (0, 10)$
Cyclic variance	$\sigma_t^2 = \sigma_0^2(1 + a \cdot \sin(\omega t))$	$\sigma_0^2 = 1, \omega = \frac{2\pi}{100}, a \in (0, 10)$
Randomly varying variance	$\sigma_t^2 = \sigma_{t-1}^2 + \eta_t, \eta_t \sim \mathcal{N}(0, \xi^2)$	$\sigma_0^2 = 1, \xi^2 \in (0, 1000)$

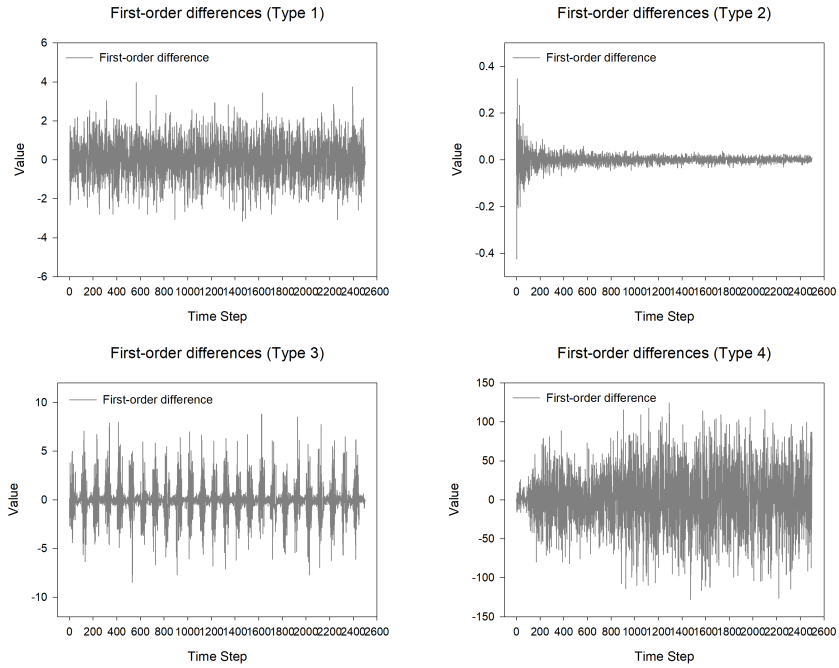


Figure 3: First-order differences of four synthetic time series: Type 1, constant variance ( $\sigma_0^2 = 1$ ); Type 2, linear variance trend ( $k = 4.95$ ); Type 3, cyclic variance ( $a = 7.77$ ); and Type 4, randomly varying variance ( $\xi^2 = 920$ ).

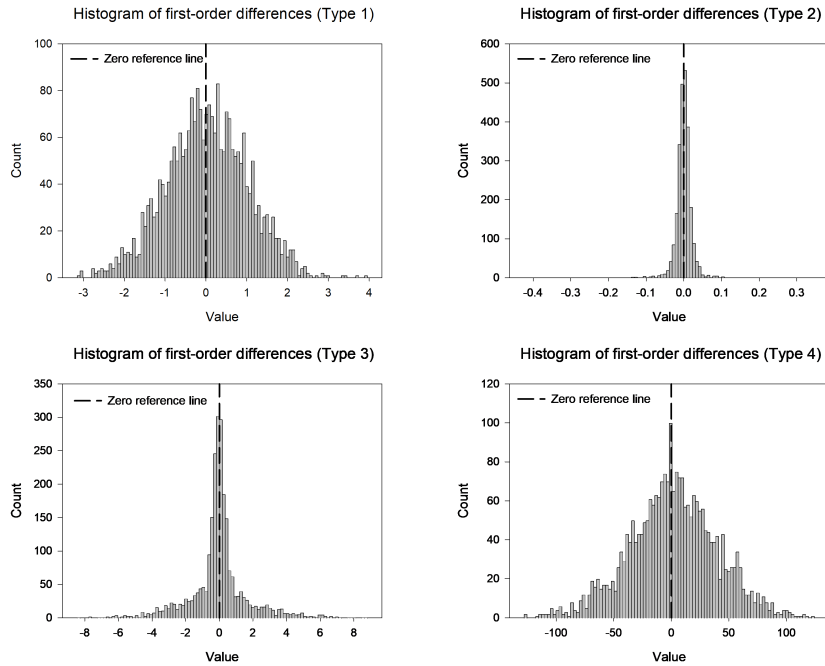


Figure 4: Histograms of first-order differences of four synthetic time series: Type 1, constant variance ( $\sigma_0^2 = 1$ ); Type 2, linear variance trend ( $k = 4.95$ ); Type 3, cyclic variance ( $a = 7.77$ ); and Type 4, randomly varying variance ( $\xi^2 = 920$ ).

For each time series, the adjusted naïve forecast on the out-of-sample set was generated via Algorithm 1, which uses the values of  $\theta$  determined by different levels of predefined directional accuracies. The performance of each adjusted naïve forecast result was evaluated using four metrics: the RMSE, MAE, MAPE, and sMAPE. The RMSE, derived from the square root of the MSE, emphasizes larger errors, which makes it suitable for identifying significant deviations in forecasts. The MAE, on the other hand, provides an interpretable measure of the average error without overpenalizing outliers. The MAPE and sMAPE normalize the errors relative to the actual values, enabling comparisons between datasets with different scales. Together, these metrics capture both absolute and relative error characteristics, ensuring a robust and balanced evaluation. The formulas for these metrics are as follows:

$$RMSE = \sqrt{\frac{1}{N} \sum_{i=1}^N (y_i - \hat{y}_i)^2}, \quad (24)$$

$$MAE = \frac{1}{N} \sum_{i=1}^N |y_i - \hat{y}_i|, \quad (25)$$

$$MAPE = \frac{100}{N} \sum_{i=1}^N \left| \frac{y_i - \hat{y}_i}{y_i} \right|, \quad (26)$$

$$sMAPE = \frac{100}{N} \sum_{i=1}^N \frac{|y_i - \hat{y}_i|}{\frac{|y_i| + |\hat{y}_i|}{2}}, \quad (27)$$

where  $N$  denotes the size of the out-of-sample set,  $\hat{y}_i$  denotes the predicted value, and  $y_i$  denotes the actual value.

To statistically test the performance of the adjusted naïve forecast, for each synthetic time series at a specified directional accuracy level, the process to generate the adjusted naïve forecast was repeated 100 times. Each repetition used a unique movement prediction sequence at the same directional accuracy level, which was generated by randomly replacing a subset of actual movements in the out-of-sample set with incorrect movements. The directional accuracy level varies in two ways: initially, it changes from 0.50 to 0.56 in increments of 0.01, and then it changes from 0.55 to 1.00 in larger increments of 0.05. This approach allows for finer granularity in the lower accuracy range, where small changes in the directional accuracy can have a significant effect on the performance of the method, while using larger steps at higher accuracy levels balances the computational efficiency. Consequently, for each synthetic time series, 100 independent values were calculated for each metric at each accuracy level.

### 3.2 Results and Analysis

Because the directional accuracy for the out-of-sample set is predefined in each simulation process, only the value of  $\bar{\epsilon}_{\text{out-of-sample}}$  needs to be estimated. Figure 5 illustrates the distribution of the values in the  $\bar{\epsilon}_{\text{set}}$ , generated on the basis of sliding windows across the first-order differences of the in-sample set. The vertical reference line in Figure 5 represents the actual  $\bar{\epsilon}_{\text{out-of-sample}}$  value of the out-of-sample set. In the four cases, the minimum value of  $\bar{\epsilon}_{\text{set}}$  is generally an underestimate of  $\bar{\epsilon}_{\text{out-of-sample}}$ , except for the second case, where the synthetic time series is a random walk with a decreasing trend of linear variance. However, the estimated value remains close to the true value. Under the assumption that directional accuracy is consistent across the in-sample and out-of-sample sets, this estimation ensures that inequality (22) is satisfied.

Furthermore, comparisons of the two types of naïve forecasts based on the four evaluation metrics at low accuracy levels are illustrated in Figures 6, 7, 8, and 9. Each box plot in each figure represents the distribution of 100 independent metric values at a specific directional accuracy level, with the metric value of the original naïve forecast shown as a reference line. According to Figure 6, at low accuracy levels, such as 0.51, the RMSE of the adjusted naïve forecast is comparable to or slightly better than that of the original naïve forecast, as shown by the proximity of the median of each box plot to the reference line. As the accuracy increased beyond 0.52, most of the RMSE values fell below the baseline.

Because the adjusted naïve forecast consistently outperforms the original naïve forecast at low accuracy levels in terms of the MAE, MAPE, and sMAPE, the Wilcoxon signed rank test was conducted to specifically evaluate whether the median differences between the RMSE values of the adjusted naïve forecast and those of the original naïve forecast significantly deviated from zero for accuracy levels ranging from 0.50–0.56 (Li and Johnson, 2014). As summarized in Table 2, at a directional accuracy level of 0.51, the adjusted naïve forecast shows mixed results with respect to statistical significance. Although significant improvements were observed over the original naïve forecast for the Type 4 series (randomly varying variance,  $p = 0.002$ ), the results for the Type 1 (constant variance,  $p = 0.915$ ), Type 2 (linear variance trend,  $p = 0.781$ ), and Type 3 (cyclic variance,  $p = 0.812$ ) series were not statistically significant, indicating that an accuracy level of 0.51 may not consistently produce meaningful improvements across all types of time series. As the

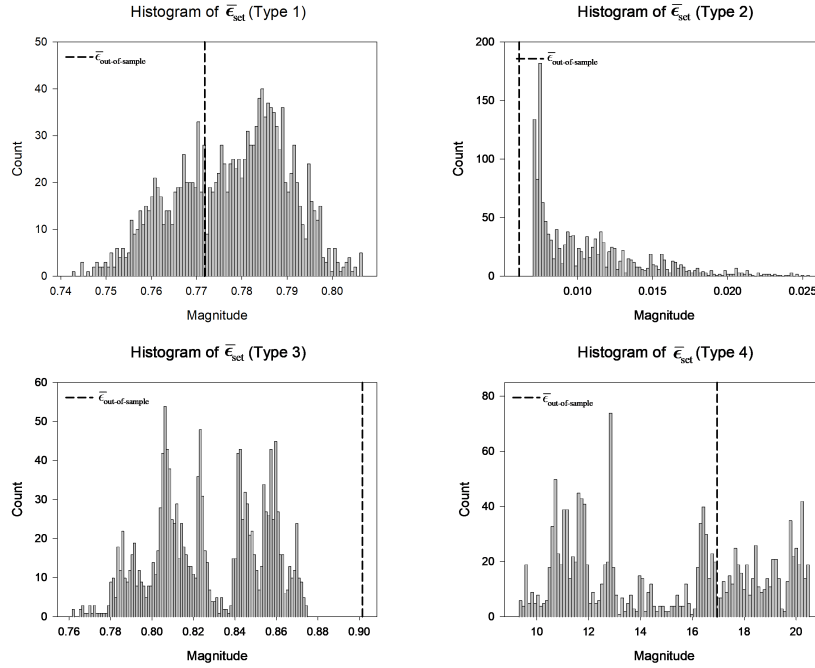


Figure 5: Comparison of the true  $\bar{\epsilon}_{\text{out-of-sample}}$  with  $\bar{\epsilon}_{\text{set}}$ : Type 1, constant variance ( $\sigma_0^2 = 1$ ); Type 2, linear variance trend ( $k = 4.95$ ); Type 3, cyclic variance ( $a = 7.77$ ); and Type 4, randomly varying variance ( $\xi^2 = 920$ ).

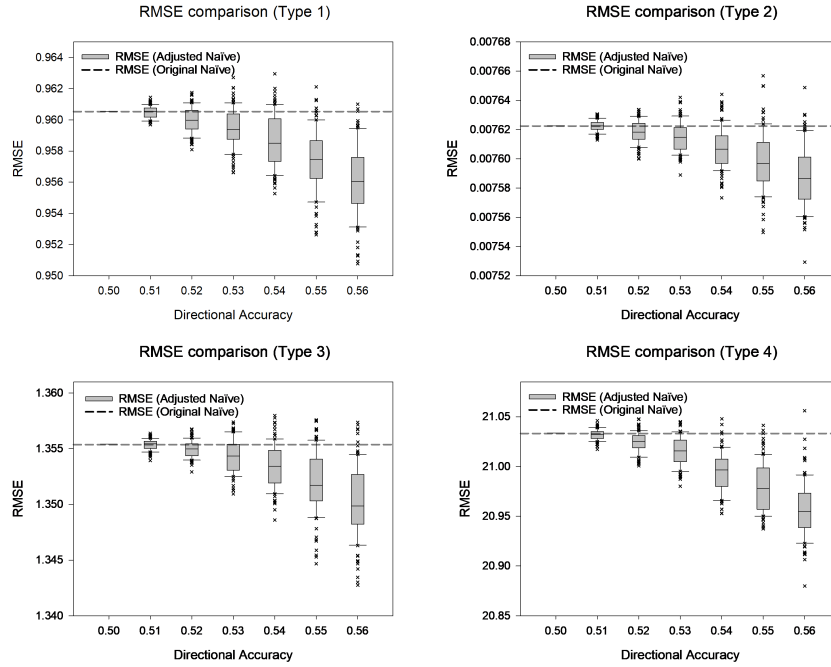


Figure 6: RMSEs of the adjusted naïve forecast across different directional accuracy levels (0.50–0.56) for four synthetic time series: Type 1, constant variance; Type 2, linear variance trend; Type 3, cyclic variance; and Type 4, randomly varying variance.

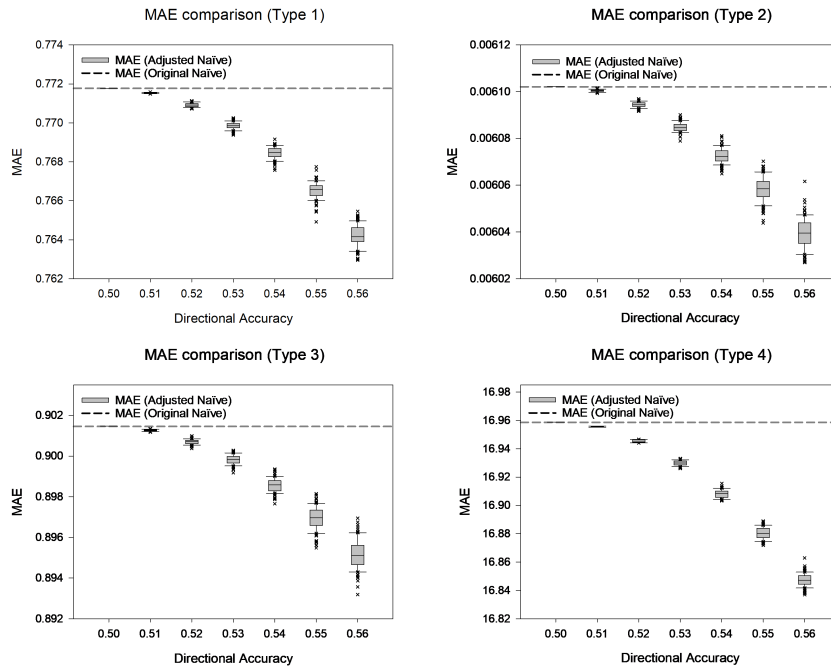


Figure 7: MAEs of the adjusted naïve forecast across different directional accuracy levels (0.50–0.56) for four synthetic time series: Type 1, constant variance; Type 2, linear variance trend; Type 3, cyclic variance; and Type 4, randomly varying variance.

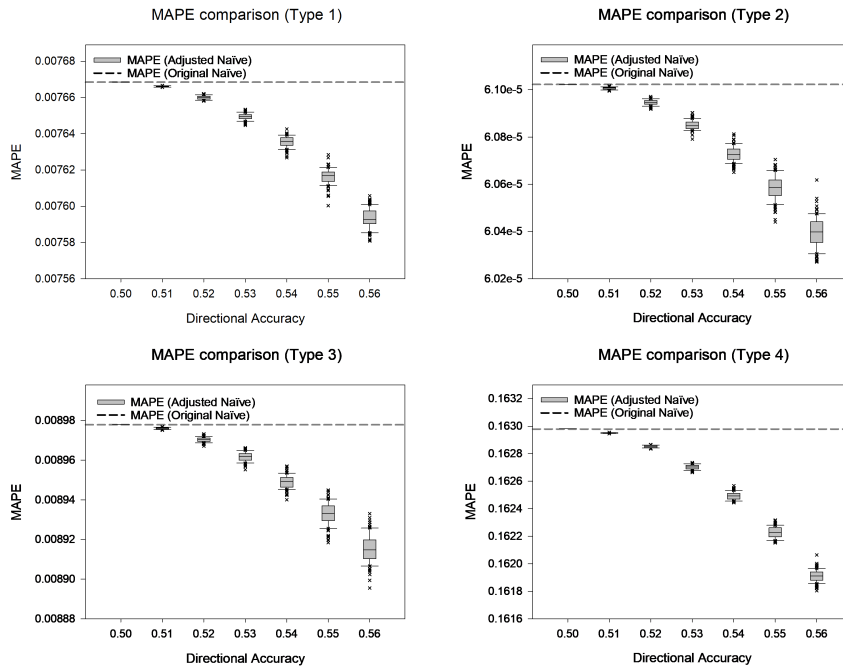


Figure 8: MAPEs of the adjusted naïve forecast across different directional accuracy levels (0.50–0.56) for four synthetic time series: Type 1, constant variance; Type 2, linear variance trend; Type 3, cyclic variance; and Type 4, randomly varying variance.

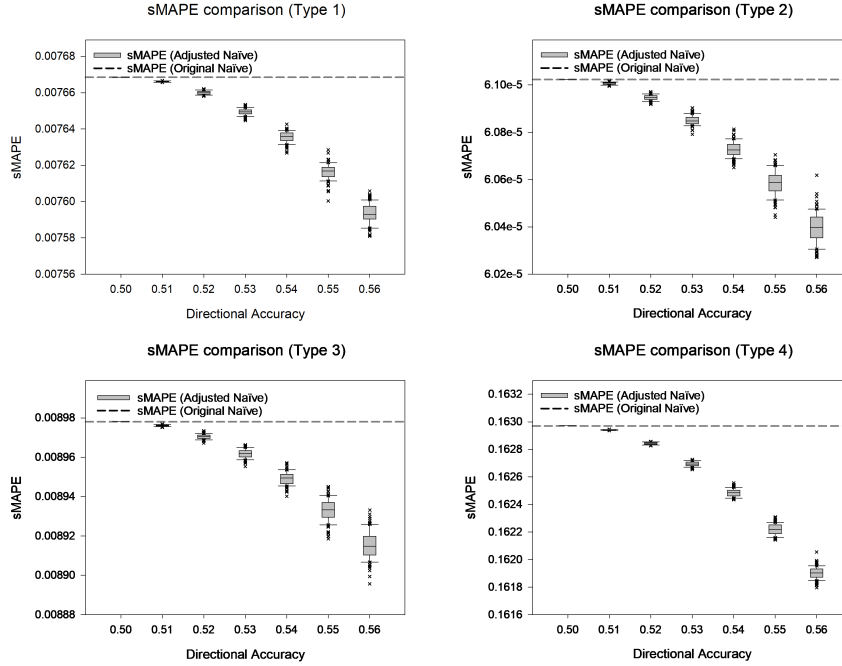


Figure 9: sMAPEs of the adjusted naïve forecast across different directional accuracy levels (0.50–0.56) for four synthetic time series: Type 1, constant variance; Type 2, linear variance trend; Type 3, cyclic variance; and Type 4, randomly varying variance.

Table 2: RMSE results of the adjusted naïve forecast across directional accuracy levels (0.50–0.56) for four synthetic time series: Type 1, constant variance; Type 2, linear variance trend; Type 3, cyclic variance; and Type 4, randomly varying variance.

Prediction	Type 1		Type 2		Type 3		Type 4	
	RMSE Range	p-value	RMSE Range	p-value	RMSE Range	p-value	RMSE Range	p-value
Original Naïve	0.961	-	0.00762	-	1.355	-	21.034	-
Acc = 0.50	0.961	-	0.00762	-	1.355	-	21.034	-
Acc = 0.51	0.960 ± 0.0004	0.915	0.00762 ± 0.000003	0.781	1.355 ± 0.0005	0.812	21.032 ± 0.0053	0.002
Acc = 0.52	0.960 ± 0.0008	<0.001	0.00762 ± 0.000007	<0.001	1.355 ± 0.0008	<0.001	21.024 ± 0.0102	<0.001
Acc = 0.53	0.959 ± 0.0012	<0.001	0.00761 ± 0.000010	<0.001	1.354 ± 0.0015	<0.001	21.015 ± 0.0144	<0.001
Acc = 0.54	0.959 ± 0.0017	<0.001	0.00761 ± 0.000014	<0.001	1.353 ± 0.0020	<0.001	20.995 ± 0.0199	<0.001
Acc = 0.55	0.957 ± 0.0020	<0.001	0.00760 ± 0.000020	<0.001	1.352 ± 0.0028	<0.001	20.979 ± 0.0244	<0.001
Acc = 0.56	0.956 ± 0.0023	<0.001	0.00758 ± 0.000021	<0.001	1.351 ± 0.0032	<0.001	20.957 ± 0.0278	<0.001

accuracy increased beyond 0.51, significant reductions in the RMSE ( $p < 0.001$ ) were observed for all types of time series, thereby demonstrating the reliability and effectiveness of the adjusted naïve forecast at higher accuracy levels.

According to Figures 10, 11, 12, and 13, at higher accuracy levels ranging from 0.55–1.00, the adjusted naïve forecast consistently outperforms the original naïve forecast in terms of the four metrics. In particular, the improvement over the original naïve forecast becomes more pronounced as the directional accuracy improves. This finding demonstrates that highly accurate movement predictions can be effectively translated into improved point forecasts in the context of forecasting random walk-like time series. However, the improvement over the original naïve forecast is limited, because the proposed method allows a random walk-like series to be predicted to a certain extent, but the predicted value cannot be infinitely close to the actual value.

In general, when the directional accuracy was 0.5, the adjusted naïve forecast did not provide an improvement over the original naïve forecast. However, as the directional accuracy increases, the performance of the adjusted naïve forecast improves. This result is consistent with the theoretical analysis of the proposed method, which highlights its robustness

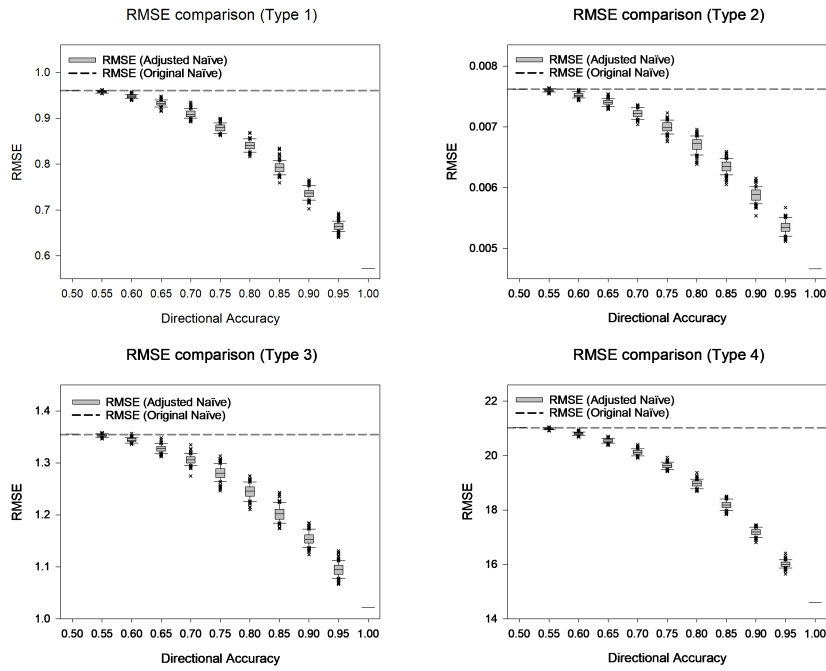


Figure 10: RMSEs of the adjusted naïve forecast across different directional accuracy levels (0.55–1.00) for four synthetic time series: Type 1, constant variance; Type 2, linear variance trend; Type 3, cyclic variance; and Type 4, randomly varying variance.

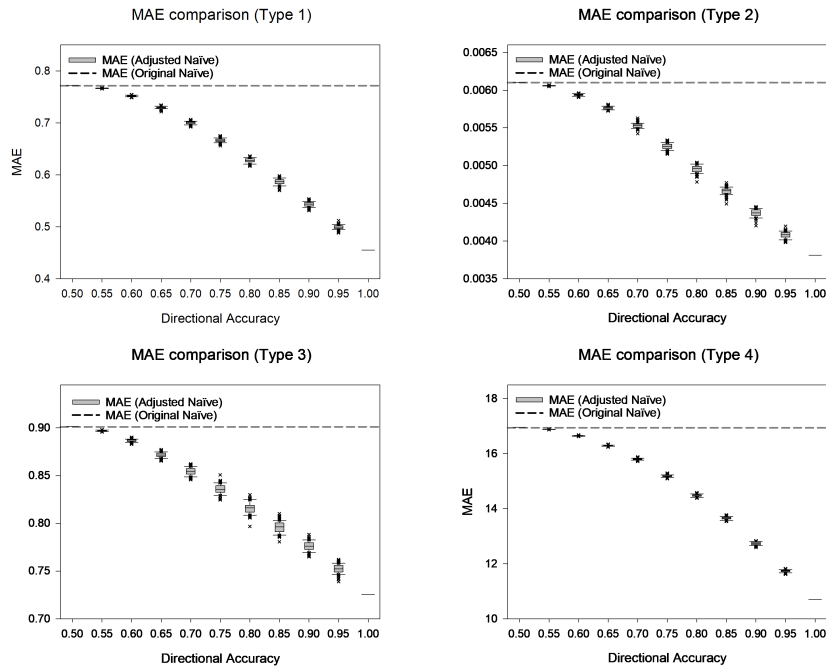


Figure 11: MAEs of the adjusted naïve forecast across different directional accuracy levels (0.55–1.00) for four synthetic time series: Type 1, constant variance; Type 2, linear variance trend; Type 3, cyclic variance; and Type 4, randomly varying variance.



## Movement-Prediction-Adjusted Naïve Forecast (ZHANG, 2025)

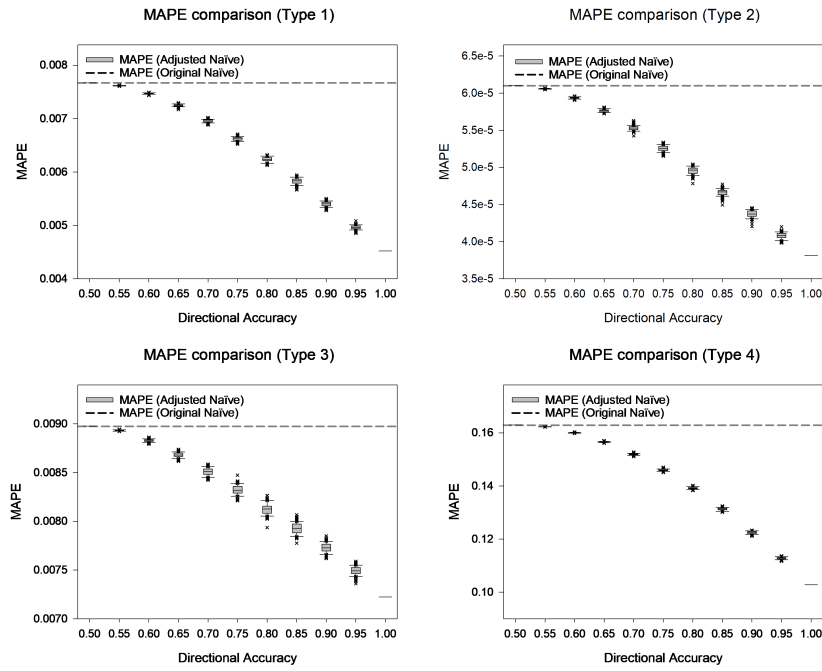


Figure 12: MAPEs of the adjusted naïve forecast across different directional accuracy levels (0.55–1.00) for four synthetic time series: Type 1, constant variance; Type 2, linear variance trend; Type 3, cyclic variance; and Type 4, randomly varying variance.

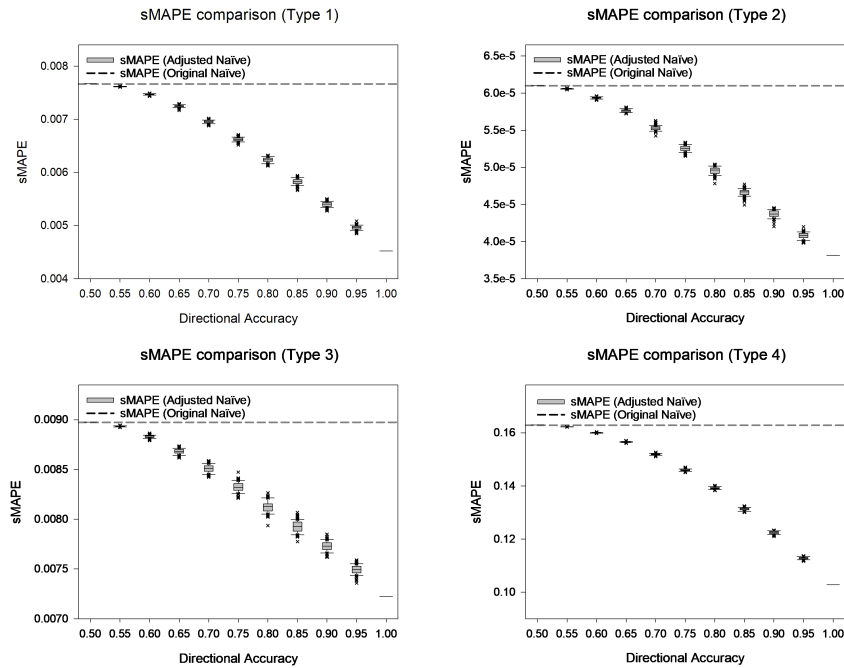


Figure 13: sMAPEs of the adjusted naïve forecast across different directional accuracy levels (0.55–1.00) for four synthetic time series: Type 1, constant variance; Type 2, linear variance trend; Type 3, cyclic variance; and Type 4, randomly varying variance.

and potential applicability to a wide range of time series that exhibit symmetric random walk characteristics, including those with homoscedasticity as well as high-volatility scenarios.

## 4 Discussion

This section discusses the implications of the findings and potential limitations of this study. First, this study demonstrates an indirect regression approach that uses only movement predictions and the original naïve forecast for a random walk-like time series. The theoretical analysis and simulation results indicate that as the directional accuracy increases, the improvement over the original naïve forecast also increases, suggesting that improving movement predictions may be more critical than developing direct regression models in this context. It also highlights a fundamental trade-off between maximizing the probability that the method outperforms the original naïve forecast and achieving a meaningful level of improvement, reflecting an inherent uncertainty in prediction tasks that purely data-driven approaches may sometimes overlook.

Second, many real-world forecasting scenarios require the integration of predictions from different data types to support decision-making (Bishop and Nasrabadi, 2006; Timmermann, 2006). However, it is difficult to combine binary and continuous forecasts. The proposed method can be regarded as a feasible approach to convert binary movement predictions into continuous point forecasts. This conversion facilitates the comprehensive use of diverse predictions and can enhance decision-making in practice.

Third, this study focuses on the theoretical predictability of random walk-like time series rather than exploiting this predictability for profit. Although certain structural properties or external signals may slightly improve movement predictions and thereby point forecasts, the forecasting result does not necessarily translate into economic gains, especially when transaction costs, market frictions, and slippage are considered.

Finally, because the aim of this study was to show how incorporating movement predictions can enhance naïve forecasts rather than how to generate movement predictions, we relied on simulations rather than real-world examples. Notably, the effectiveness of the adjusted naïve forecast depends on the consistent directional accuracy across different segments of the time series. Movement prediction models prone to overfitting may show a decline in directional accuracy on the out-of-sample set, limiting the actual improvement over the naïve forecast using the proposed method.

## 5 Conclusion

This study introduces a movement-prediction-adjusted naïve forecast, which is a linear combination of movement prediction and the original naïve forecast, in the challenging context of forecasting time series that exhibit symmetric random walk characteristics. The weight of the movement term is determined by two parameters: one reflecting the directional accuracy and the other representing the mean absolute increment. The theoretical analysis of the proposed method explains how movement prediction can enhance point forecasting for a random walk-like series. In addition to presenting the relationship between the directional accuracy and the method's improvement over the original naïve baseline, it also reveals the source of uncertainty in these prediction tasks, which comes from the relationship between the actual and estimated values of the parameters. Furthermore, the simulation results demonstrate that the adjusted naïve forecast can achieve statistically significant improvements over the original naïve forecast, even with directional accuracies slightly greater than 0.50. These findings highlight the significant potential of using movement predictions to address the inherent challenges of point forecasting in a random walk-like time series.

There are several avenues for further research on the foundation of this study. First, while this research focuses on time series with symmetric random walk characteristics, future work could explore applying this movement prediction-based method to time series with nonsymmetric random walk properties, potentially broadening its applicability. Second, it is worth exploring whether the proposed forecasting method can be generalized beyond the one-dimensional case, as many real-world variables exhibit random walk behavior in a high-dimensional space. Moreover, the proposed method uses a fixed increment for simplicity. However, adapting this increment based on the availability of new data may provide more dynamic and accurate forecasts. Investigating how the increments can be adapted and whether such adaptive increments can further refine the forecasting accuracy represents a promising direction for future research.

## Acknowledgments

This study did not receive any specific grants from funding agencies in the public, commercial, or not-for-profit sectors.

## References

- Baker, M. and Wurgler, J. (2007). Investor sentiment in the stock market. *Journal of economic perspectives*, 21(2):129–151.
- Barberis, N., Shleifer, A., and Vishny, R. (1998). A model of investor sentiment. *Journal of financial economics*, 49(3):307–343.
- Beck, N., Dovern, J., and Vogl, S. (2025). Mind the naive forecast! a rigorous evaluation of forecasting models for time series with low predictability. *Applied Intelligence*, 55(6):395.
- Beraha, M., Metelli, A. M., Papini, M., Tirinzoni, A., and Restelli, M. (2019). Feature selection via mutual information: New theoretical insights. In *2019 international joint conference on neural networks (IJCNN)*, pages 1–9. IEEE.
- Bishop and Nasrabadi (2006). *Pattern recognition and machine learning*. Springer.
- Bustos, O. and Pomares-Quimbaya, A. (2020). Stock market movement forecast: A systematic review. *Expert Systems with Applications*, 156:113464.
- Cover, T. M. and Thomas, J. A. (2012). *Elements of Information Theory*. John Wiley & Sons.
- Crutchfield, J. P. and Feldman, D. P. (2003). Regularities unseen, randomness observed: Levels of entropy convergence. *Chaos: An Interdisciplinary Journal of Nonlinear Science*, 13(1):25–54.
- De Bondt, W. F. and Thaler, R. (1985). Does the stock market overreact? *The Journal of finance*, 40(3):793–805.
- De Gooijer, J. G. et al. (2017). *Elements of nonlinear time series analysis and forecasting*, volume 37. Springer.
- Ellwanger and Snudden (2023). Forecasts of the real price of oil revisited: Do they beat the random walk? *Journal of Banking & Finance*, 154:106962.
- Fama, E. F. (1970). Efficient capital markets. *Journal of finance*, 25(2):383–417.
- Gigerenzer, G. and Brighton, H. (2009). Homo heuristicus: Why biased minds make better inferences. *Topics in cognitive science*, 1(1):107–143.
- Granger, C. W. (1969). Investigating causal relations by econometric models and cross-spectral methods. *Econometrica: journal of the Econometric Society*, pages 424–438.
- Guyon, I. and Elisseeff, A. (2003). An introduction to variable and feature selection. *Journal of machine learning research*, 3(Mar):1157–1182.
- Hamilton, J. D. (2020). *Time series analysis*. Princeton university press.
- Hewamalage, H., Ackermann, K., and Bergmeir, C. (2023). Forecast evaluation for data scientists: common pitfalls and best practices. *Data Mining and Knowledge Discovery*, 37(2):788–832.
- Ibe (2014). *Fundamentals of applied probability and random processes*. Academic Press.
- Ircio, J., Lojo, A., Mori, U., and Lozano, J. A. (2020). Mutual information based feature subset selection in multivariate time series classification. *Pattern Recognition*, 108:107525.
- John, G. H., Kohavi, R., and Pfleger, K. (1994). Irrelevant features and the subset selection problem. In *Machine learning proceedings 1994*, pages 121–129. Elsevier.
- Kilian, L. and Taylor, M. P. (2003). Why is it so difficult to beat the random walk forecast of exchange rates? *Journal of International Economics*, 60(1):85–107.
- Kraskov, A., Stögbauer, H., and Grassberger, P. (2004). Estimating mutual information. *Phys. Rev. E*, 69:066138.
- Laplace, P.-S. (2012). *Pierre-Simon Laplace philosophical essay on probabilities: translated from the fifth french edition of 1825 with notes by the translator*, volume 13. Springer Science & Business Media.
- Lee, C. M., Shleifer, A., and Thaler, R. H. (1991). Investor sentiment and the closed-end fund puzzle. *The journal of finance*, 46(1):75–109.
- Li and Johnson (2014). Wilcoxon’s signed-rank statistic: What null hypothesis and why it matters. *Pharmaceutical Statistics*, 13(5):281–285.
- Ma, Y., Mao, R., Lin, Q., Wu, P., and Cambria, E. (2023). Multi-source aggregated classification for stock price movement prediction. *Information Fusion*, 91:515–528.
- Moosa (2013). Why is it so difficult to outperform the random walk in exchange rate forecasting? *Applied Economics*, pages 3340–3346.
- Moosa and Burns (2014). The unbeatable random walk in exchange rate forecasting: Reality or myth? *Journal of Macroeconomics*, 40:69–81.

- Moosa and Burns (2016). The random walk as a forecasting benchmark: drift or no drift? *Applied Economics*, 48(43):4131–4142.
- Petropoulos, F., Apiletti, D., Assimakopoulos, V., Babai, M. Z., Barrow, D. K., Taieb, S. B., Bergmeir, C., Bessa, R. J., Bijak, J., Boylan, J. E., et al. (2022). Forecasting: theory and practice. *International Journal of Forecasting*, 38(3):705–871.
- Sezer, O. B., Gudelek, M. U., and Ozbayoglu, A. M. (2020). Financial time series forecasting with deep learning: A systematic literature review: 2005–2019. *Applied soft computing*, 90:106181.
- Stock, J. H. and Watson, M. W. (2002). Forecasting using principal components from a large number of predictors. *Journal of the American statistical association*, 97(460):1167–1179.
- Taylor (2008). *Modelling financial time series*. World Scientific.
- Thakkar and Chaudhari (2021). Fusion in stock market prediction: A decade survey on the necessity, recent developments, and potential future directions. *Information Fusion*, 65:95–107.
- Timmermann, A. (2006). Forecast combinations. *Handbook of economic forecasting*, 1:135–196.
- Verleysen, M. and François, D. (2005). The curse of dimensionality in data mining and time series prediction. In *International work-conference on artificial neural networks*, pages 758–770. Springer.
- Wang, H., Xie, Z., Chiu, D. K., and Ho, K. K. (2025). Multimodal market information fusion for stock price trend prediction in the pharmaceutical sector. *Applied Intelligence*, 55(1):1–27.
- Weng, B., Ahmed, M. A., and Megahed, F. M. (2017). Stock market one-day ahead movement prediction using disparate data sources. *Expert Systems with Applications*, 79:153–163.
- Zeng, A., Chen, M., Zhang, L., and Xu, Q. (2023). Are transformers effective for time series forecasting? In *Proceedings of the AAAI conference on artificial intelligence*, volume 37, pages 11121–11128.